

A highly detailed FEM volume conductor model based on the ICBM152 average head template for EEG source imaging and TCS targeting*

Stefan Haufe¹, Yu Huang², and Lucas C. Parra²

Abstract—In electroencephalographic (EEG) source imaging as well as in transcranial current stimulation (TCS), it is common to model the head using either three-shell boundary element (BEM) or more accurate finite element (FEM) volume conductor models. Since building FEMs is computationally demanding and labor intensive, they are often extensively reused as templates even for subjects with mismatching anatomies. BEMs can in principle be used to efficiently build individual volume conductor models; however, the limiting factor for such individualization are the high acquisition costs of structural magnetic resonance images. Here, we build a highly detailed (0.5 mm³ resolution, 6 tissue type segmentation, 231 electrodes) FEM based on the ICBM152 template, a nonlinear average of 152 adult human heads, which we call ICBM-NY. We show that, through more realistic electrical modeling, our model is similarly accurate as individual BEMs. Moreover, through using an unbiased population average, our model is also more accurate than FEMs built from mismatching individual anatomies. Our model is made available in Matlab format.

I. INTRODUCTION

Today, a multitude of tools are available to ‘read and write the brain’ from outside the head. Brain imaging technologies such as electroencephalography (EEG) allow one to track the activity of neuronal populations with millisecond precision. Conversely, transcranial current stimulation (TCS) can be used to induce changes in neuronal firing patterns by injecting electrical currents into the skin. What is common to these technologies is that they rely on a volume conductor model of the human head and its internal structures in order to establish the connection between the active/activated brain structures and the sensors/stimulators located on the scalp, where the precision of the model determines the localization error made by EEG inverse solutions, and the error made when targeting certain brain structures using TCS.

As head anatomies vary greatly across the population, individual structural information from magnetic resonance imaging (MRI) is in general required to build precise volume conductor models. However, the acquisition of individual structural MR images is not always possible, and generally comes at a high cost.

*This work was supported by a Marie Curie International Outgoing Fellowship (grant No. PEOF-GA-2013-625991) within the 7th European Community Framework Programme.

¹Stefan Haufe is with the Laboratory for Intelligent Imaging and Neural Computing, Columbia University, New York, NY 10027, USA, and with the Machine Learning Dept., Technische Universität Berlin, 10587 Berlin, Germany. stefan.haufe@tu-berlin.de

²Yu Huang and Lucas C. Parra are with the Neural Engineering Lab, The City College of the City University of New York, New York, NY 10031, USA. yhuang16@citymail.cuny.edu, parra@ccny.cuny.edu

If individual structural information is available, a boundary element electrical model (BEM) can be built relatively easily and with a high degree of automation using several freely available software packages. Three-shell BEMs are currently the predominant approach in EEG sources imaging. Here, smoothed versions of the outer edges of brain, skull and skin are extracted from structural MR images. Finite element models (FEM), which are predominant in transcranial current stimulation (TCS) research, are more accurate than BEMs since they allow more detailed modeling of tissue types with complex shapes such as the highly-conducting cerebrospinal fluid (CSF) [12]. They are, however, more resource-consuming than BEMs due to their high computational complexity and the lack of fully automated segmentation pipelines for more than three tissue types. It is therefore common in TCS studies to build an FEM from an ‘arbitrary’ individual anatomy, and use it as a template for all subjects throughout a study.

Here we reason that, while it may remain infeasible to compute highly accurate FEMs in individual anatomies at the scale of larger studies, an improvement may already be achieved by replacing arbitrary templates with an unbiased population average. This approach is feasible, as, through advances in nonlinear co-registration, average anatomies have recently reached a level of detail comparable to that of the best individual templates. We built a highly precise FEM based on the ICBM152 head, which is a nonlinear average of the heads of 152 adults [2], and which is already widely used as an anatomical template by the neuroimaging community. Our model, called ICBM-NY or ‘New York Head’, is made available under <http://neuralengr.com/NYHead>.

The model was evaluated on four individual heads, for which we also built precise FEMs serving as a ‘ground truth’. We investigated how well the electrical leadfields in these heads are approximated using our FEM of the ICBM152 head. Moreover, we compared the approximation quality with that of BEM and spherical harmonics expansion (SHE) models computed on the matching individual anatomy, with FEMs of other (mismatching) individual anatomies, and with a BEM of an ‘individualized’ ICBM152 geometry that is warped to the electrode positions of the correctly matching anatomy.

II. METHODS

A. Structural data and coordinate systems

We used the ICBM152 template as the anatomical basis of our electrical model. The 2009b version of the ICBM152 provides highly detailed (0.5 mm³ isotropic resolution) T1-weighted structural images of an average adult head, which are

the result of a nonlinear registration of the structural images of 152 individual subjects [2]. We here use the left-right symmetric version of the template. Note that the ICBM152 head is by construction aligned with the MNI152 linear average template defining the Montreal Neurological Institute (MNI) coordinate system.

In addition to the ICBM152 head, we acquired MR images (1 mm³ isotropic resolution, T1-weighted) of four individuals (denoted INDV1–4, male, age range 27–45) at a magnetic field of 3 T. All images were rotated into their ‘native’ space defined by the locations of the anterior and posterior commissures, and an interhemispheric point. Notice here that the MNI space is the native space of the ICBM152 head.

Using the Statistical Parametric Mapping (SPM8) package (Wellcome Trust Centre for Neuroimaging, London, UK) for Matlab (The Mathworks, Natick, MA, USA), 12-parameter affine transforms from each individual subject’s native space to MNI space were calculated. These transforms were later used to match cortical locations in different anatomies. They were not used to spatially normalize MR images.

B. Segmentation and electrode placement

MR images of individual subjects INDV1–4 were segmented by a probabilistic segmentation routine implemented in SPM [1]. Using the Chris-Rorden Tissue Probability Map (CR-TPM) developed in [7], each head was segmented into six tissue types: gray matter (GM), white matter (WM), CSF, skull, scalp and air cavities. An in-house Matlab script was used to correct for segmentation errors conducted by SPM8 (see [7] for details).

A segmentation for the ICBM152 template was developed from three sources: the older 6th generation version of the ICBM152 non-linear template [4], the newer 2009b symmetric version of the ICBM152 non-linear template mentioned above [2], and the CR-TPM template [7]. Both versions of the ICBM152 head were segmented using the procedure described above. Since the ICBM152 v2009b is characterized by a higher resolution and better image quality in the brain region, but poorer quality in the non-brain region compared to the ICBM152 v6, the non-brain tissues (CSF, skull, scalp, air) obtained from ICBM152 v6 were registered to the voxel space of ICBM152 v2009 using the ‘Coregister’ routine of SPM8. Moreover, since the field of view of both ICBM152 templates only reaches down to the nose, while the CR-TPM covers the whole head, the CR-TPM was also registered to the voxel space of ICBM152 v2009. Therefore, we fused the brain (GM, WM) obtained from ICBM152 v2009b with the non-brain tissues obtained from ICBM152 v6 and the lower head obtained from CR-TPM. This provided a new averaged, high-resolution (0.5 mm³), whole-head model referred to as ICBM152. Anatomical errors from the registration process were manually corrected in ScanIP 4.2 (Simpleware Ltd, Exeter, UK).

For all heads, $M = 231$ electrodes were placed on the scalp surface automatically following the international 10-05 system [9]. This was performed using a custom Matlab script described in [7]. Specifically, we used a subset of 165

electrode locations defined in the 10-05 system, which was augmented by two additional rows of electrodes below the ears, and four additional electrodes around the neck.

C. Finite element modeling

A finite element model was generated for each head using ScanIP (+ScanFE Module) with adaptive irregular element sizes (ScanFE-Free algorithm). In order to avoid clotting of nearby electrodes on the scalp surface, which would artificially make the scalp surface highly conductive, the electrodes and the underlying gel were not physically modeled. Electrodes were thus placed directly on the scalp surface. The Laplace equation $\nabla \cdot (\sigma \mathbf{E}) = 0$ was solved in Abaqus 6.11 (SIMULIA, Providence, RI, USA) for the electric field distribution \mathbf{E} in the head. Each tissue type was assigned a conductivity as in [7]. The boundary conditions were set to: insulated on the scalp surface, grounded on the cathode surface, and 1 A/m² inward current density on the anode surface.

For each head, the model was solved for all possible bipolar electrode configurations with one fixed reference electrode (Iz). Given the reciprocity principle [10], the relationship of externally applied currents to fields inside the head is equal to the ‘leadfield’ typically used in the EEG community, namely, the voltages generated at the scalp electrodes with a dipole placed inside the head. The leadfield in the GM was extracted and calibrated to correspond to a 1 mA current injection from the scalp surface. Note that our overall model implements the guidelines for precise FE modeling of the head formulated by [12].

D. Boundary element and spherical harmonics modeling

Using the ‘Morphologist’ pipeline of BrainVISA¹, high-resolution ($\sim 75\,000$ nodes) meshes of the cortical surface were obtained for all five heads from their T1-weighted MR images. Figure 1 shows the extracted cortical surfaces. Note that the smoothed versions shown in the right panel of the figure are solely used for plotting. Surfaces meshes of the brain, skull and scalp compartments comprising 1 922 nodes each were extracted using the Brainstorm package [11]. Within this 3-shell geometry, the EEG forward problem was solved using the boundary element method (BEM) [5] as well as spherical harmonics expansions (SHE) of the electric leadfields [8]. The electrical conductivities used for the brain, skull and scalp compartments were $\sigma_1 = 0.33$ S/m, $\sigma_2 = 0.041$ S/m and $\sigma_3 = 0.33$ S/m, respectively.

In addition to the ICBM152 and INDV1–4 heads, four warped versions of the ICBM152 template were constructed. In each of these, the ICBM152 head surface was nonlinearly morphed to fit the electrodes placed on one of the four individual heads. Note that this is possible in practice using 3D digitization hardware without requiring individual structural MRI data. The estimated warping transformations were subsequently applied to all precomputed surfaces of the ICBM152 head. Leadfields were computed in these warped anatomies using BEM, giving rise to four ‘individualized’ (as

¹<http://brainvisa.info/>

opposed to ‘individual’, which refers to the use of structural MR images) volume conductor models.

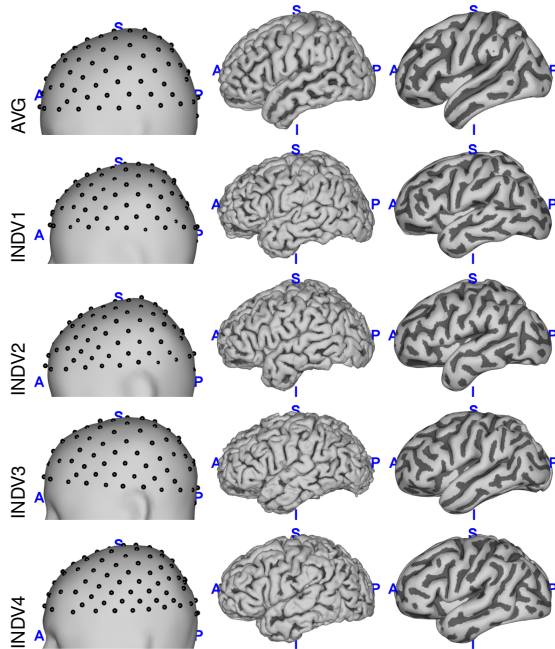


Fig. 1. The ICBM152 average head (AVG) and four individual heads (INDV1–4). Left: head (outer shell of the BEM) surface with 108 electrodes placed. Center: cortical surface. Right: smoothed cortical surface. Cortical sulci are marked in dark color.

E. Assessment of leadfield approximation accuracy

We treat the FEM calculated in the correctly matching individual anatomy as the ‘ground truth’. We assessed deviations from this ground truth for the leadfield computed for either of the following models: a BEM or SHE electrical model using the matching individual anatomy (denoted as TRUE BEM and TRUE SHE), the FEM of another individual’s anatomy (OTH INDV FEM), the FEM of the ICBM152 average head (AVG FEM), or a ‘individualized’ BEM of the ICBM152 anatomy (WARP AVG BEM). The analysis was carried out on a subset of $\sim 10\,000$ locations covering the entire cortical surface. Furthermore, a subset of 108 electrode locations was selected for the simulations. The distribution of these electrodes across the scalp is shown in Figure 1 for all heads. All leadfields were re-referenced to the common average of the selected channels.

Given a point on the cortical surface in the target anatomy, corresponding locations in the approximate anatomy were determined as follows. For TRUE BEM and TRUE SHE the correctly matching anatomy is used, and no mapping is needed. For WARP AVG BEM, the approximate anatomy is by definition in the native space of the target anatomy through the SPM warping. Here, matching points are found as the ones with shortest Euclidean distance to the target location. For AVG FEM, the ICBM152 head is warped from MNI space into the target head’s native space through the transformation described in Section II-A. For OTH INDV FEM, the same was achieved by combining the native-to-MNI transformation

of the approximate anatomy and the MNI-to-native transformation of the target anatomy. In the target’s native space, matching locations are determined by Euclidean distance.

At each target location, the leadfield is compared to the leadfield at the matching location in the approximate anatomy in two ways. First, the relative mean-squared error (MSE) is computed. For the $3 \times M$ target and approximation leadfields \mathbf{L}_t and \mathbf{L}_a , the relative MSE is defined as $\|\mathbf{L}_t - \mathbf{L}_a\|_F^2 / \|\mathbf{L}_t\|_F^2$, where $\|\cdot\|_F^2$ is the sum of the squared entries of a matrix. Second, the angle between the subspaces spanned by \mathbf{L}_t and \mathbf{L}_a is computed using Matlab’s `subspace` command. The subspace angle is independent of the scale of the leadfields, as well as of rotations within 3D space. It is therefore a suitable measure of *subspace correlation*. Here we consider these subspace angles normalized to the interval $[0, 1]$.

Notice that low MSE are required to achieve the desired intensity along the anticipated spatial direction at a target in a TCS setting, while high subspace correlation is the prerequisite for correctly localizing EEG sources, where the strength and direction of the estimated sources is of minor importance.

III. RESULTS

Figure 2 depicts the results of the leadfield approximation assessment. In the upper panel, the distributions shown are pooled over the four individual heads serving as target anatomies. Results reported for mismatched individual model anatomies (OTH INDV FEM) are moreover averaged over the three heads serving as models (e.g., INDV2–4 when INDV1 is the target anatomy). According to the relative MSE, our ICBM152 model (AVG FEM) outperforms all competing models, while in terms of subspace correlation, it outperforms mismatched individual anatomies (OTH INDV FEM), as well as a spherical harmonics model of the matching anatomy, while being on par with a BEM of the ICBM152 template warped externally to the matching individual anatomy. Here, AVG FEM is only outperformed by a BEM computed in the correctly matching individual anatomy (TRUE INDV BEM).

The lower panels of figure 2 depict topographic distributions of the approximation errors made for the representative target anatomy INDV1. Here it can be seen that the ICBM152 model approximates the INDV1 model least favorably in the left temporal lobe. In terms of the relative MSE, TRUE INDV BEM performs worst with high errors in central superficial areas, possibly due to numerical inaccuracies along the interfaces between the brain and skull shells. This is in contrast to the subspace correlation criterion, according to which TRUE INDV BEM performs the best. Generally, leadfield correlations drop dramatically in deeper areas such as the tips of the temporal lobes for models based on three-shell approximations (WARP AVG BEM, TRUE INDV BEM and TRUE INDV SHE) as compared to FEMs. Mismatched individual models moreover generally provide a poor leadfield approximation according to both criteria.

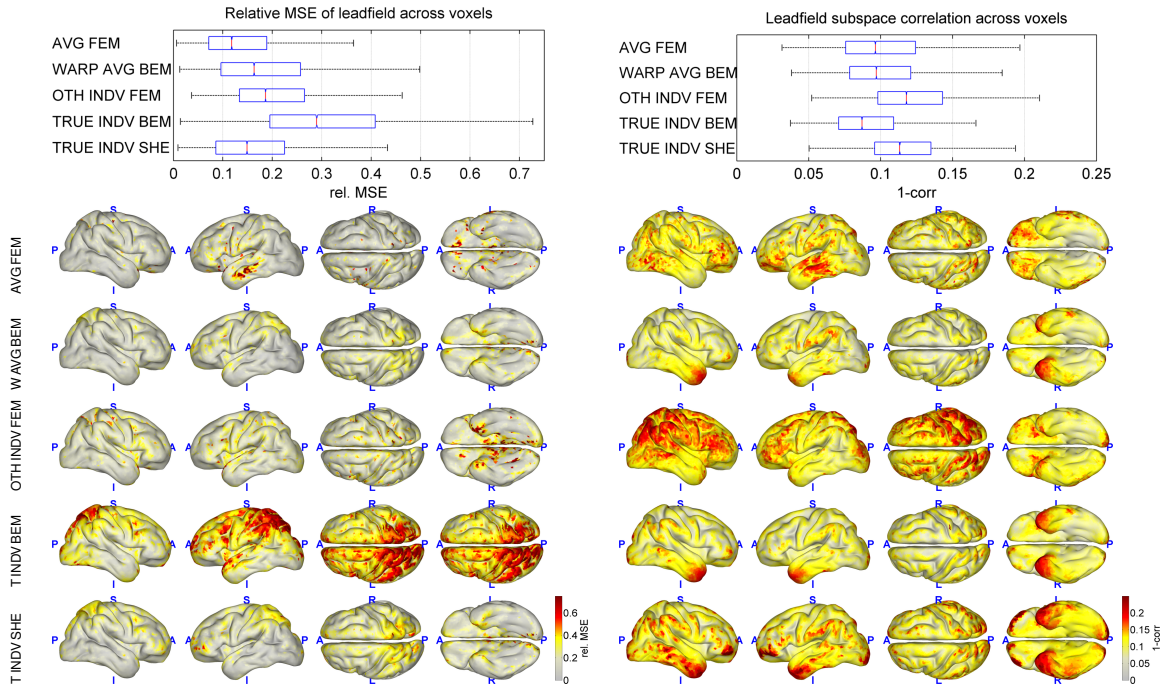


Fig. 2. Relative mean-squared error (MSE) incurred and subspace correlation achieved across cortical locations when approximating the ‘true leadfield’ (the leadfield computed using FEM in the target anatomy) by a leadfield computed either using a mismatched anatomy or a simpler electrical model in the correctly matching anatomy. AVG FEM: approximation by the proposed FEM of the ICBM152 average head. WARP AVG BEM: approximation through a BEM using a warped version of the ICBM152 template whose head surface has been fitted to the electrode positions of the correctly matching head. OTH INDV FEM: approximation by FEMs of three different mismatched individual anatomies. TRUE INDV BEM and TRUE INDV SHE: approximation by BEM and SHE models using the correctly matching anatomy, which is often not available in practice. Upper panels: Median, 25th and 75th percentile, and most extreme values attained across the cortical locations of all four individual subjects INDV1–4. Lower panels: topographic distributions of the approximation errors for subject INDV1. Smaller values indicate better approximation performance.

IV. CONCLUSION

We present the ICBM-NY head model, detailed FEM of the ICBM152b nonlinear average of the human head, implementing the guidelines of [12]. Our results indicate that our model is a viable alternative to individual and individualized BEMs, as well as FEMs of ‘arbitrary’ individuals, in EEG source imaging and TCS targeting studies. Another intended use of our model are simulations, where we expect it to become a standard model for testing EEG source imaging methodologies (and subsequent analyses), as well as TCS targeting protocols, prior to real-world application [6], [14].

Current limitations and future research: The current evaluation was based on models of the heads of four Caucasian males serving as the ‘ground truth’. Whether the proposed model is a good approximation for the general population must be studied using larger numbers of more diverse target heads. Furthermore, while our model aims to improve EEG source localization and TCS targeting accuracy, the analyses presented here were limited to comparing leadfields across cortical locations. A quantitative analysis in terms immediately relevant to the EEG and TCS communities is left to our full-length paper [13].

ACKNOWLEDGMENT

We thank D. Brooks, C. Wolters, A. Gramfort, G. Nolte, M. Bikson, M. Dannhauer, and D. Miklody for fruitful discussions.

REFERENCES

- [1] J. Ashburner and K. J. Friston. Unified segmentation. *Neuroimage*, 26(3):839–851, 2005.
- [2] V. Fonov et al. . Unbiased average age-appropriate atlases for pediatric studies. *NeuroImage*, 54(1):313–327, 2011.
- [3] K.J. Friston et al., editors. *Statistical Parametric Mapping: The Analysis of Functional Brain Images*. Academic Press, 2007.
- [4] G. Grabner et al. . Symmetric atlasing and model based segmentation: an application to the hippocampus in older adults. *Med Image Comput Comput Assist Interv*, 9(Pt 2):58–66, 2006.
- [5] A. Gramfort et al. . OpenMEEG: opensource software for quasistatic bioelectromagnetics. *Biomed Eng Online*, 9:45, 2010.
- [6] S. Haufe et al. . A critical assessment of connectivity measures for EEG data: a simulation study. *NeuroImage*, 64:120–133, 2012.
- [7] Y. Huang et al. . Automated MRI segmentation for individualized modeling of current flow in the human head. *J Neural Eng*, 10(6):066004, 2013.
- [8] G. Nolte and G. Dassios. Analytic expansion of the EEG lead field for realistic volume conductors. *Phys Med Biol*, 50:3807–3823, 2005.
- [9] R. Oostenveld and P. Praamstra. The five percent electrode system for high-resolution EEG and ERP measurements. *Clin Neurophysiol*, 112:713–719, 2001.
- [10] S. Rush and D. A. Driscoll. EEG electrode sensitivity—an application of reciprocity. *IEEE Trans Biomed Eng*, 16(1):15–22, 1969.
- [11] F. Tadel et al. . Brainstorm: a user-friendly application for MEG/EEG analysis. *Comput Intell Neurosci*, 2011:879716, 2011.
- [12] J. Vorwerk et al. . A guideline for head volume conductor modeling in EEG and MEG. *NeuroImage*, 100(0):590 – 607, 2014.
- [13] Y. Huang et al. . ICBM-NY – A highly detailed volume conductor model for EEG source localization and TCS targeting. *NeuroImage*, 2015. Submitted.
- [14] S. Haufe. An extendable simulation framework for benchmarking EEG-based brain connectivity estimation methodologies. *Conf Proc IEEE Eng Med Biol Soc (EMBC)*, 2015. In Press.